Conference Paper, Published Version

Ahmed, Ashraf A.; Elleboudy, Azza M.

Effect of Sheetpile Configuration on Seepage beneath Hydraulic Structures

Effect of Sheetpile Configuration on Seepage beneath Hydraulic Structures

Ashraf A. Ahmed[1] and Azza M. Elleboudy[2]

[1]Associate Professor, Department of Civil Engineering, Faculty of Engineering, Benha University, 108 Shobra St., Cairo 11629, Egypt; PH (202) 2672-1922; email: ashraf.elkholy@gmail.com
[2]Professor, Department of Civil Engineering, Faculty of Engineering, Benha University, 108 Shobra St., Cairo 11629, Egypt; PH (202) 2526-4224; email: prof.azza@feng.bu.edu.eg

ABSTRACT

This paper investigates the influence of various sheetpile configurations on the seepage losses, the uplift force on downstream apron of floor, and the exit gradient at the end toe of the apron. A computer program, utilizing the finite element method and based on the fixed mesh approach, was used to locate the free surface of water. The model was applied to investigate seepage below and around a hydraulic structure. Several configurations of the sheetpile driven under the structure were analyzed. Results showed that when the sheetpile confined the downstream apron of the floor from all sides, it has dramatically reduced the exit gradient. In return, this was accompanied by some increase in the uplift pressure force acting on the structure. Other configurations that needed more sheetpile material had little effect on the uplift force and exit gradient.

KEYWORDS: Unconfined seepage; Uplift force; Exit gradient; Finite element; Seepage losses.

INTRODUCTION

Hydraulic structures built over pervious soil strata should be secured against uplift forces acting on the floor of the structure and against the phenomenon of piping. For this purpose, design engineers always provide the floor of the structure with one or more sheetpile to reduce the uplift force and exit gradient at the downstream toe of the apron (Cedergren, 1989). This is because the consequence of piping and erosion, resulted by letting the exit gradient approaches its critical value, can be very severe and may lead to complete failure of the structure (Griffiths and Fenton, 1998).

Researchers follow a conventional analysis when studying seepage flow under hydraulic structures: only the flow beneath the floor has been considered with complete disregard to the water seeping through the banks of the canal. The main reason for this is because most of these analyses are two-dimensional (2D). Even though in three-dimensional (3D) analysis (e.g. Ahmed et al., 2007a; Griffiths and Fenton, 1997, 1998), the water seeping through the banks was overlooked. This leads to limitations in the investigation of sheetpile configuration. The sheetpile position,

considered in most of the previous studies, is one or more sheetpile driven beneath the floor of the structure and extends laterally in the out-of-plane direction across the floor width.

The main objective of the current research was to investigate the influence of different sheetpile configurations on seepage losses, the uplift force, and the exit gradient at the end toe of the apron. The canal width/differential head ratio was constant. In each case, the 3D results were compared with that obtained from the 2D analysis.

MATHEMATICAL BACKGROUND

Residual Flow Procedure (RFP)

The RFP presented herein, which was used to locate the free surface, follows closely Bathe and Khoshgoftaar (1979), Desai and Li (1983), and Desai and Baseghi (1988). The partial differential equation that governs steady incompressible fluid flow through porous medium can be written as:

$$div\,(k\ \mathrm{grad}\phi) = 0.0 \tag{1}$$

where, k= hydraulic conductivity of the medium , $_{\phi} = P/\gamma + Z$= total fluid head, P/γ is the pressure head, Z is the elevation head, and γ is unit weight of fluid.

The pseudo-functional ,U ,for the steady state flow can be expressed as:

$$U = \frac{1}{2}\iiint_{v} k\left[\left(\frac{\partial\phi}{\partial x}\right)^2 + \left(\frac{\partial\phi}{\partial y}\right)^2 + \left(\frac{\partial\phi}{\partial z}\right)^2\right] dx\,dy\,dz \tag{2}$$

Applying the RFP yields the element equations:

$$\left[k_S\right]^e \{q\} = \{Q_r\}^e \tag{3}$$

Where $[k_s]^e$ is the element hydraulic conductivity matrix at saturation, $\{q\}$ is the vector of nodal fluid heads of element, and $\{Q_r\}^e$ is the element residual flow vector composed as,

$$\{Q_r\}^e = \left[k_{us}\right]^e \{q\} \tag{4}$$

Where $[k_{us}]^e$ is the unsaturated hydraulic conductivity matrix. The assembly over elements yields:

$$\left[K_S\right]\{r\} = \{R_r\} \quad \text{on the entire domain} \tag{5}$$

Where $[K_s]$ is the overall hydraulic conductivity matrix at saturation, $\{r\}$ is the overall nodal fluid head vector, and $\{R_r\}$ is the overall residual flow vector. Eq. 5 is a system of nonlinear equations.

For the free surface flow through the banks, the hydraulic conductivity was taken according to Bathe and Khoshgoftaar (1979):

$$k = \begin{cases} k_s & P \geq 0 \\ k_s / 1000 & P < 0 \end{cases} \tag{6}$$

A detailed model description, verification, and applications can be found in Ahmed et al. (2007a, b)

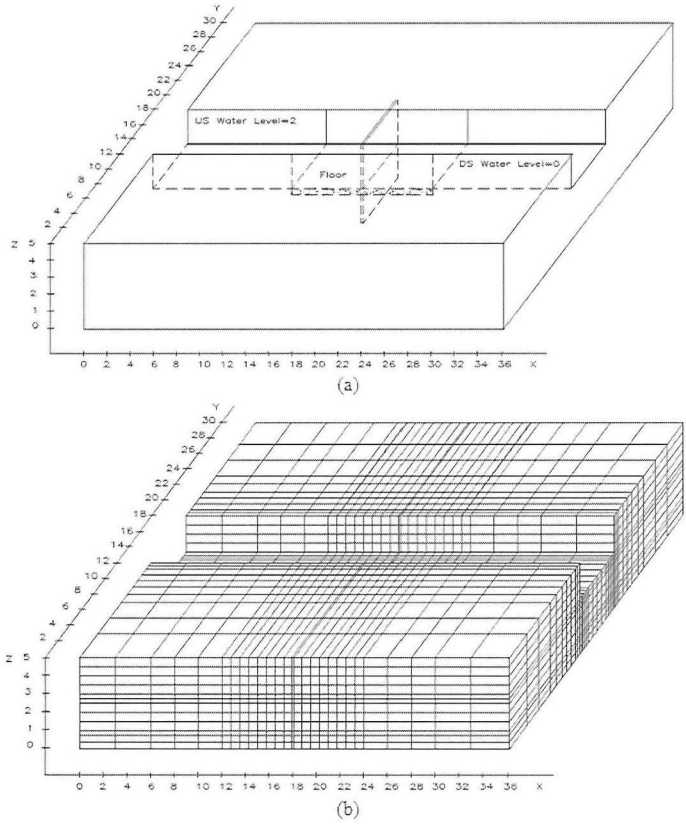

Figure 1. Isometric view and finite element mesh for the application problem.

APPLICATION PROBLEM AND ANALYSIS PROCEDURE

Figure 1-a shows an isometric view of the problem: a hydraulic structure resting on a pervious homogenous isotropic soil of depth 3 m, and hydraulic conductivity $5x10^{-4}$ m/sec. A sheetpile of penetration depth 2 m is driven underneath the structure. The length of the modeled zone was 36 m, considering two vertical impervious boundaries 18 m upstream and downstream the sheetpile. No appreciable change was observed in results when the domain length was extended beyond 36 m. The banks of the canal extended 12 m each side and its top level was 2 m above the bed level of the canal. The floor of the structure was 12 m in length and extended 6m across the canal width. The side retaining walls of the structure rose up to the bank level. The seepage flow occurs due to a differential head of 2 m between the upstream and the downstream sides of the structure. Figure 1-b shows the finite element mesh used in the analysis. The total number of nodes was 10780 and the total number of elements was 9072.

The problem was studied by considering different values of the width of the sheetpile driven under the floor. These cases are W/B = 1, 2, 3 and 5, where B is the width of the canal (6 m), and W is the total width of the sheetpile. In all cases, the sheetpile was symmetric about the canal centerline and extended vertically up to the top level of the banks. The problem was then studied for another two cases. In the first case, the sheetpile confined the downstream floor from three sides then in the second case, the sheetpile confined the downstream floor from all sides. Figure 2 illustrates the various cases.

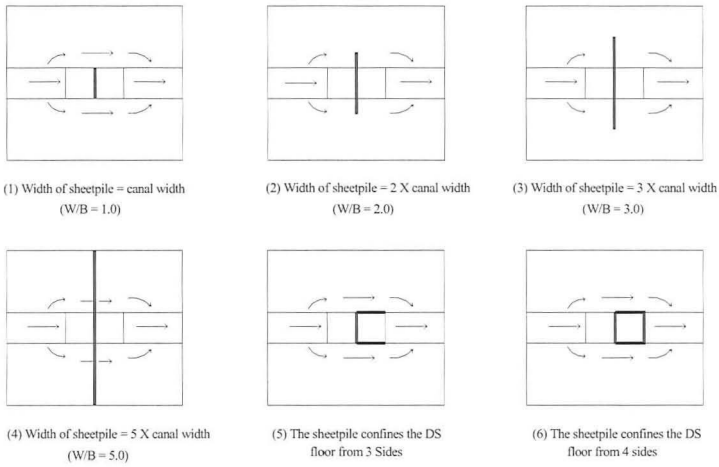

Figure 2. Different arrangements for sheetpile driven under the structure.

BOUNDARY CONDITIONS

The bed level of the canal was taken as the reference level. The bed and vertical sides of the canal on the upstream side were modeled as prescribed head boundaries where the head equaled 2.0 m. The bed of the canal on the downstream side was also modeled as prescribed head boundary with zero head. The exit surface was represented along the downstream vertical sides of the canal since flow could possibly exit anywhere along these faces. All the external vertical boundaries, the bottom boundary, the floor, and the retaining walls were modeled as impermeable boundaries.

RESULTS AND DISCUSSION

Figure 3 shows the change in exit gradient at the end of the downstream floor apron along the channel width. The exit gradient attained its maximum value at the canal edges not at the centerline, as it has traditionally been thought. It can also be noticed that there was a significant reduction on the exit gradient when the sheetpile confined the downstream apron from all sides. Moreover, when the sheetpile confined the downstream apron from three sides only as in case 5, it introduced no appreciable change in the exit gradient compared with case 1 although the length of the sheetpile used was 3-times more. The same applies to case 4; there was no appreciable change in the exit gradient compared with case 1 although the length of the sheetpile used in case 4 was 5-times more.

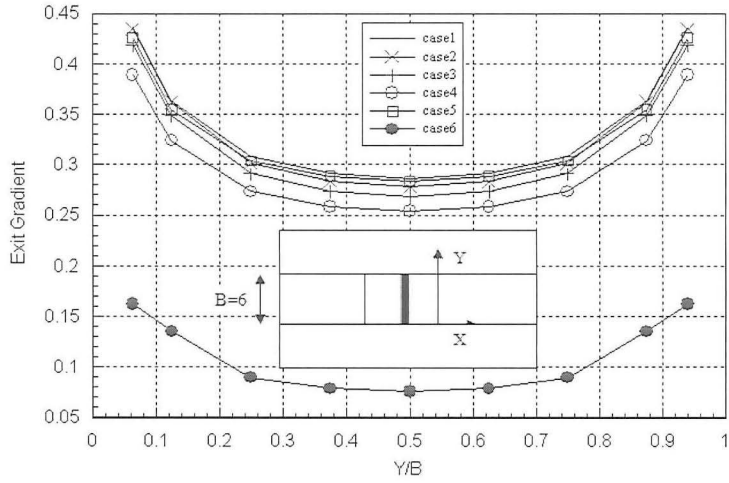

Figure3. Change in exit gradient along the canal width.

Figure 4 depicts the change of the flow rate, the uplift force under the downstream floor apron, and the exit gradient measured at the edge of the canal, for the different cases. The vertical axis represents the flow rate, the exit gradient, and the uplift force of the modeled 3-D cases normalized to their values obtained from the 2-D solution of this problem. The flow rate was calculated by considering only the part flowing under the floor of the structure. This was done to facilitate comparison between the different 3-D cases and the 2-D solution. The normalized values of the flow rate were less than unity. It is because part of the seeping water flows through the banks. The flow rate steadily increased as the W/B value increased. This is because the open space of the banks was gradually decreased as the width of the sheetpile increased. When the sheetpile covered the entire width of the modeled domain (case 4), the conditions approached the 2-D solution. Obviously, the effect of increasing the sheetpile width did not introduce a noticeable change in the flow rate.

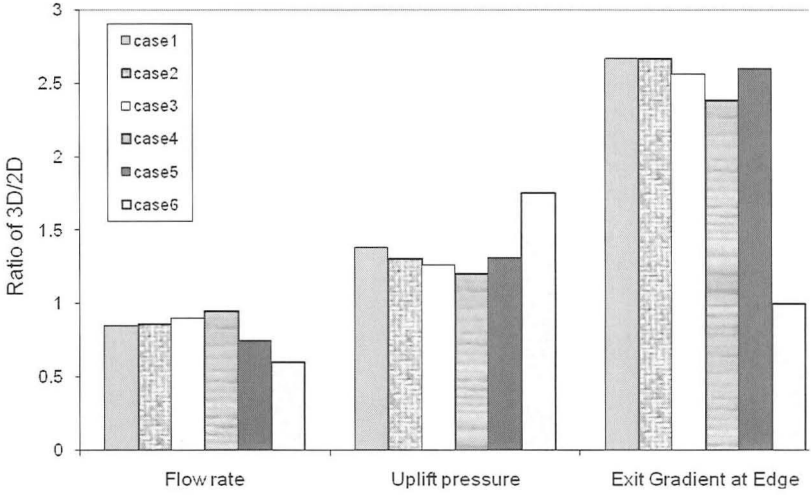

Figure 4. Change of flow rate, uplift pressure, and exit gradient with sheetpile configurations.

The uplift force increased to reach 140% for case1 and 175 % for case 6 relative to their corresponding values obtained from the 2-D solution (Fig. 4). This increase in the value of uplift pressure in case 6 than in case 1 is because the way the water has to travel under the floor of the structure is longer for case 6 than case 1. This can be clarified by referring to the distribution of the uplift pressure under the floor according to the method of Bligh (Leliavesly, 1965). The uplift pressure distribution is shown in Figure 5-a for case 1, and in Figure 5-b for case 6. The value

of the uplift pressure h_2 at the end toe is greater in case 6 than in case 1, while it has same value h_1 at the middle sheetpile. In other words, the area the uplift pressure acted upon, which determines the uplift force, is greater for case 6 than case 1. Obviously in Figure 4, the effect of increasing the sheetpile width (cases 1 to 5) did not introduce a significant reduction in the uplift force.

The relative value of the exit gradient increased markedly to reach about 270% for the case W/B=1. For all cases, with the exception of case 6, the value of the exit gradient is very high compared to the corresponding value obtained from the 2-D solution of the same problem. This illustrates that values obtained from the 2-D solution are sometimes in great error. The reason of this increase in the exit gradient produced from the 3-D solution is because of the water flow through the banks, which is not considered in the 2-D solution.

When the sheetpile confined the downstream floor apron from all sides (case 6), the exit gradient was dramatically reduced. This dramatic reduction in the exit gradient is attributed to increasing the length through which water percolates, while the differential water head is constant. The practical consequence of this reduction in the exit gradient is clear, that the safety of the structure against piping and percolation increases. Obviously, if the sheetpile was driven under the floor as in case 6, it is more effective than other cases, such as case 4, although less sheetpile material is used in case 6 than in case 4.

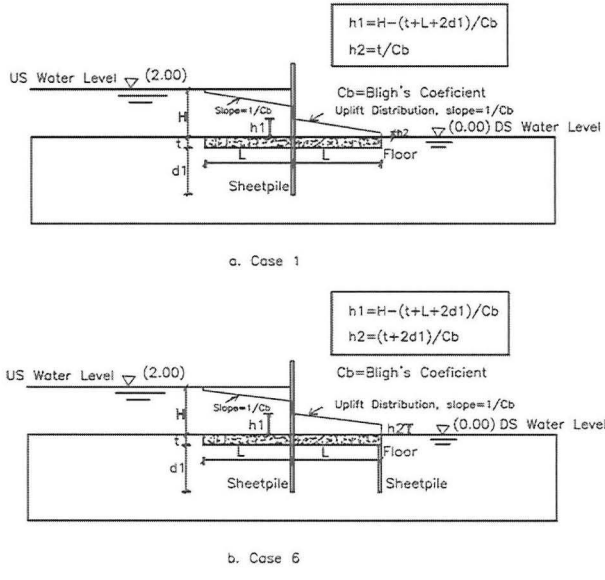

Figure 5. Change of exit uplift force with different sheetpile arrangements.

CONCLUSIONS

A number of numerical analyses were carried out to study the influence of different sheetpile configurations, constructed beneath the floor of a hydraulic structure, on seepage losses, uplift force, and exit gradient. It was observed that extending the sheetpile laterally through the banks of the canal has no appreciable influence on either uplift force acting on the structure or the exit gradient at the end toe of the floor. It only caused much more consumption of the sheetpile material with no noticeable gained benefits. It was also found that driving a sheetpile under a hydraulic structure that surrounds the downstream floor apron from all sides, has greatly reduced the exit gradient at the end toe of the floor. However, this was accompanied with some increase in the uplift force.

REFERENCES

Ahmed A. A., Soliman , A. M., and Bazaraa, A. S. (2007a). "3-D steady analysis of leaky hydraulic structures: 1. Leaky sheetpiles." *Journal of Engineering and Applied Science* 54 (2):141-157.

Ahmed A. A., Soliman , A. M., and Bazaraa, A. S. (2007b). "3-D Steady analysis of leaky hydraulic structures: 2. Leaky dams." *Journal of Engineering and applied Science* 54 (3): 289-302.

Bathe, K. J., and Khoshgoftaar, M. R. (1979). "Finite element free surface seepage analysis without mesh iteration." *Int. J. Numer. Analyt. Meth. Geomech.* 3: 13-22.

Cedergren, H. R. (1989). "Seepage, Drainage, and Flow Nets." 3rd Edition, New York: Wiley.

Desai, C. S., and Li, G. C. (1983). "A residual flow procedure and application for free surface flow in porous media." *Adv. Water Resour.* 6: 27-35.

Desai,C. S., and Baseghi, B. (1988). "Theory and verification of residual flow procedure for 3-D free surface seepage." *Adv. Water Resour.* 11: 192-203.

Griffiths, D. V., and Fenton, G. A. (1997). "Three-dimensional seepage through spatially random soil." *J. Geotechnical and Geoenvironmental Engrg.*123: 153-160.

Griffiths, D. V., and Fenton, G. A. (1998). "Probabilistic analysis of exit gradients due to steady seepage." *J. Geotechnical and Geoenvironmental Engrg.*124: 789-797.

Leliavesly S. (1965). *Design of Dams for Percolation and Erosion.* Chapman and Hall, London.